02.2

Search for axioelectric effect in Kr atoms for solar axions

© E.F. Bubnov[1], Yu.M. Gavrilyuk[2], A.N. Gangapshev[2], A.V. Derbin[1], I.S. Drachnev[1], V.V. Kazalov[2], V.V. Kuzminov[2], V.N. Muratova[1], D.A. Tekueva[2], E.V. Unzhakov[1], S.P. Yakimenko[2]

[1] St. Petersburg Nuclear Physics Institute, National Research Center Kurchatov Institute, Gatchina, Russia
[2] Institute for Nuclear Research, Russian Academy of Sciences, Troitsk, Moscow, Russia
E-mail: derbin_av@pnpi.nrcki.ru

Received December 6, 2023
Revised December 6, 2023
Accepted December 8, 2023

A search for the axioelectric effect in krypton atoms for solar axions has been performed. The gaseous proportional chamber installed in a low- background setup located at underground facility of Baksan Neutrino Observatory (INR RAS) was used. As a result, new limits were obtained on the coupling constant of an axion with an electron ($|g_{Ae}| \leqslant 4.9 \cdot 10^{-11}$) and on the product of the coupling constant with an electron and a photon ($|g_{Ae}g_{A\gamma}| \leqslant 1.6 \cdot 10^{-19}\,\mathrm{GeV}^{-1}$), all for 90% c.l.

Keywords: solar axions,dark matter, axion-like particles.

DOI: 10.21883/0000000000

The detection of axions (hypothetical [1], but highly sought-after particles that both solve the problem of CP-conservation in strong interactions and serve as well-motivated dark matter particle candidates) relies on the effective coupling constants of axons with photons $g_{A\gamma}$, electrons g_{Ae}, and nucleons g_{AN} [2,3]. An in-depth review of theoretical and experimental axion research was provided in [4]. The key reactions proposed for detection are the conversion of axions into photons in a magnetic field or in the field of a nucleus, the decay of an axion into two photons, the Compton conversion, and the axioelectric effect. The axioelectric effect (AE), which is examined in the present study, is similar to the photoelectric effect (PE). An axion vanishes as a result of reaction, producing a free electron and subsequent characteristic X-ray radiation of an atom. The AE cross section is directly proportional to the PE cross section and constant g_{Ae}^2, and the number of AE events depends on the flux and the spectrum of axions incident on a detector.

Axions may be produced on the Sun in a number of processes: bremsstrahlung radiation $e + Z \to Z + e + A$, Compton process $\gamma + e \to e + A$, and atomic recombination and deexcitation processes. The fluxes and spectra of these axions are proportional to g_{Ae}^2 and were calculated in [5–9]. In our calculations, we used the tabular $(d\Phi_{Ae}/dE_A)$ axion spectrum from [9], which includes additionally the axion emission in atomic processes.

Axions are produced in conversion of thermal photons in an electromagnetic field of plasma (Primakoff effect), and their flux is governed by $g_{A\gamma}^2$. The energy spectrum of axions produced as a result of this effect is specified by the following parameterization [10]:

$$\frac{d\Phi_{A\gamma}}{dE_A} = 6.02 \cdot 10^{30} g_{A\gamma}^2 E_A^{2.481} e^{-E_A/1.205}. \qquad (1)$$

Here, the $d\Phi_{A\gamma}/dE_A$ flux is given in units of $\mathrm{cm}^{-2} \cdot \mathrm{s}^{-1} \cdot \mathrm{keV}^{-1}$, energy E_A is in keV, and $g_{A\gamma}$ is in units of GeV^{-1}.

AE cross section σ_{ae} is proportional to PE cross section σ_{pe} and constant g_{Ae} [11]:

$$\sigma_{ae}(E_A, m_A) = \sigma_{pe} \frac{3 g_{Ae}^2 E_A^2}{16\pi\alpha m_e^2 \beta_A} \left(1 - \frac{\beta_A^{2/3}}{3}\right), \qquad (2)$$

where $\alpha = 1/137$ is the fine structure constant, m_e is the electron mass, and $\beta_A = p_A/E_A$ is the axion velocity. The AE and PE cross sections for krypton are shown as functions of energy in Fig. 1 for $g_{Ae} = 1$ and axion mass $m_A = 0$.

The spectrum of detected energy of an ejected electron, Auger electrons, and X-ray radiation takes the form

$$\frac{dN}{dE} = \sigma_{ae}(E_A, m_A) \left[\frac{d\Phi_{Ae}}{dE_A} + \frac{d\Phi_{A\gamma}}{dE_A}\right]. \qquad (3)$$

The expected Kr detector spectra for two sources of solar axions $d\Phi_{Ae}/dE_A$ and $d\Phi_{A\gamma}/dE_A$ associated with constants g_{Ae} and $g_{A\gamma}$ are shown by curves *3* and *4* in Fig. 1 (right scale). These spectra were plotted in units of $\mathrm{kg}^{-1} \cdot \mathrm{year}^{-1} \cdot \mathrm{keV}^{-1}$ for $m_A = 0$, $g_{Ae} = 10^{-11}$, and $g_{A\gamma} = 10^{-10}\,\mathrm{GeV}^{-1}$.

To compare it to an experimentally measured spectrum, expression (3) needs to be averaged with the use of the detector response function. The number of detected axions should depend on the number of krypton atoms in a target, the measurement time, and the detector efficiency, and the probability of observation of a spectrum shape corresponding to the axioelectric effect is set by the background level of the experimental setup.

A large gaseous proportional chamber filled with krypton enriched to 99% in ^{83}Kr was used to detect an electron, X-ray quanta, and Auger electrons produced as a result of

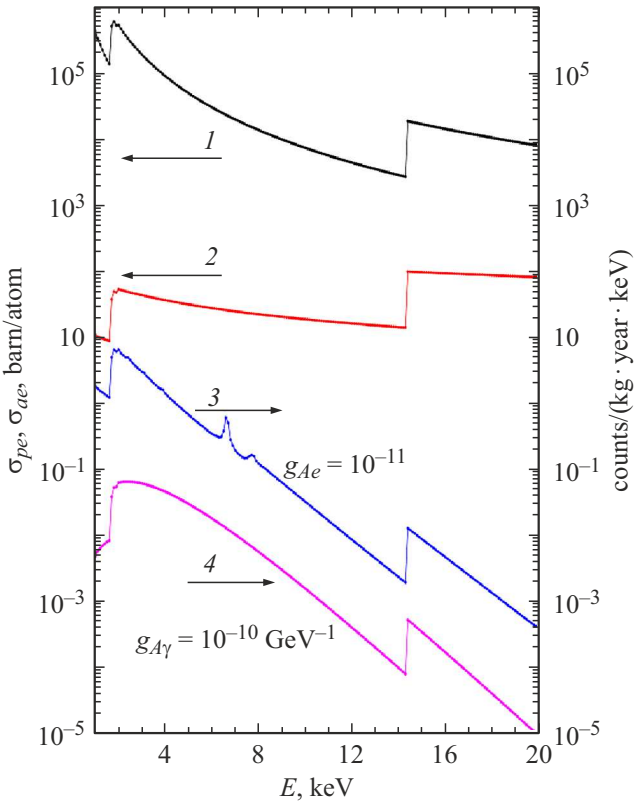

Figure 1. PE (*1*) and AE (*2*) cross sections for a Kr atom at $g_{Ae} = 1$ and $m_A = 0$ (left scale) and expected Kr detector spectra at $g_{Ae} = 10^{-11}$ (*3*) and $g_{A\gamma} = 10^{-10}\,\mathrm{GeV}^{-1}$ (*4*) (right scale).

AE. The chamber was installed within a low-background setup located in the underground laboratory of Baksan Neutrino Observatory (Institute for Nuclear Research, Russian Academy of Sciences) where an experimental search for resonance absorption of solar axions by ^{83}Kr nuclei is being carried out [12,13]. The low-background setup is positioned at a depth of 4900 m.w.e. (meter water equivalent). The muon flux at this depth is $2.60 \pm 0.09\,\mathrm{m}^{-2} \cdot \mathrm{day}^{-1}$. The cylindrical chamber is made of copper and surrounded by passive copper, lead, and polyethylene shielding. A gold-plated tungsten wire stretching along the cylinder axis serves as the anode. The overall chamber volume is 10.8 l; an anode diameter enlargement for suppression of the influence of end effects on charge collection reduces the working volume to 8.8 l. The chamber is filled with krypton under a pressure of 1.8 bar. The mass of isotope ^{83}Kr within the working chamber volume is 58 g.

The pulse shape is digitized at a frequency of 12.5 MHz. The pulse rise time provides an opportunity to select near-cathode events. The ratio of amplitudes of the primary ionization pulse and the pulse of secondary photoemission from the cathode allows one to determine the position of an event along the anode axis and select events from the central part of the detector. The energy resolution of the chamber at 10 keV is $\sigma = 420$ eV. The experimental setup was characterized in detail in our earlier studies [12,13].

The gaseous chamber spectrum measured in 777 days of live time is shown in Fig. 2. Two well-pronounced peaks are seen in it. The peak with an energy of 8 keV corresponds to characteristic X-ray radiation of copper (the chamber body material). The second peak is attributable to EC decays of long-lived isotope ^{81}Kr. X-ray krypton and bromine quanta, which emerge from the inactive region of the gaseous chamber, produce an additional contribution to broadening of the second peak.

The energy resolution of the detector allowed us to perform long-measurements starting from the threshold at 4 keV. The response function of a Kr detector for electrons and photons is approximated well within the examined energy interval by a Gaussian curve. The measured spectrum within the 4–20 keV interval was fitted with a function for continuous background $F_{bkg}(E)$ and two Gaussian peaks with all three of their parameters (position, variance, and amplitude) being free. The function characterizing continuous background featured a constant background component and an exponential background dependence with two parameters: $F_{bkg}(E) = a + b\exp\big(-c(E-4)\big)$. Thus, a total of nine parameters were varied.

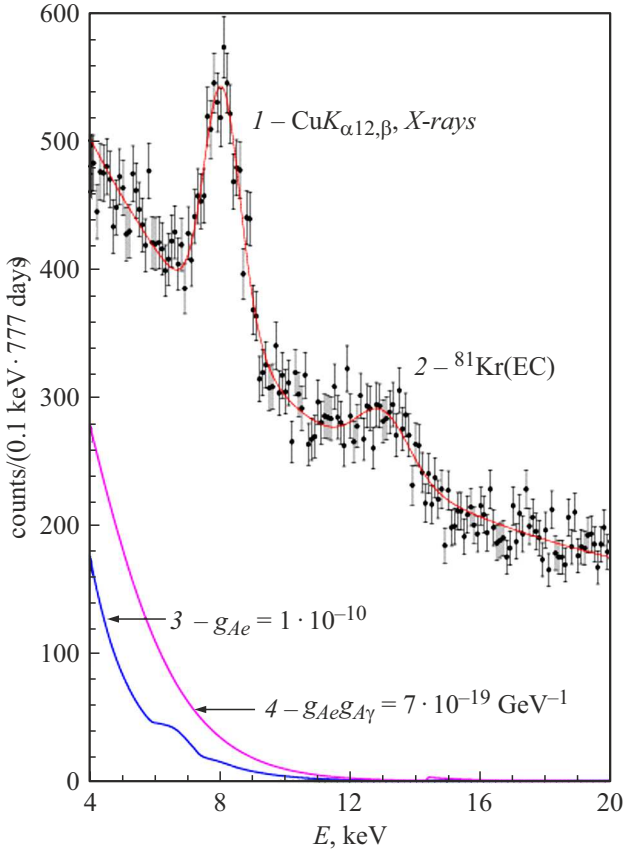

Figure 2. Kr chamber spectrum and results of fitting with the theoretical shape. *1* — Copper X-ray radiation peaks; *2* — peak associated with the decay of ^{81}Kr and X-ray radiation of Kr and Br atoms; *3* — expected AE spectrum for $g_{Ae} = 10^{-10}$; *4* — expected spectrum of Primakoff axions for $g_{Ae}g_{A\gamma} = 7 \cdot 10^{-19}\,\mathrm{GeV}^{-1}$.

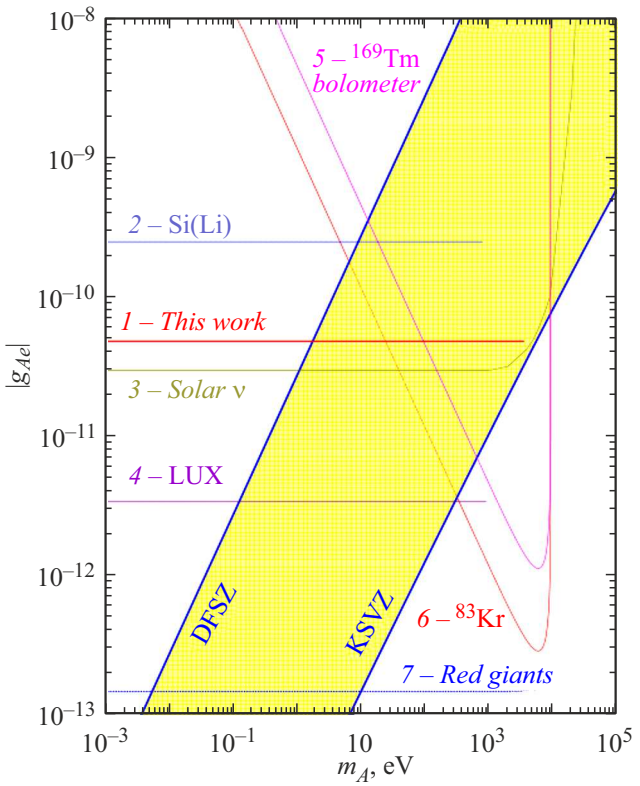

Figure 3. Upper limits on $|g_{Ae}|$ obtained in the present study (*1*) in comparison with the results of other experiments: *2* — Si(Li) detector [15]; *3* — solar neutrino data [6]; *4* — LUX experiment [16]; *5* and *6* — resonance absorption of axions by ^{169}Tm [17] and ^{83}Kr [18] nuclei, respectively; *7* — astrophysical constraints [19]. The region of possible values of parameters g_{Ae} and m_A in the DFSZ and KSVZ axion models is indicated.

A spectrum calculated in accordance with (3), which had the shape corresponding to the one expected from AE, was also added to the fitting function. The cases of solar axion flux production associated exclusively with constant g_{Ae} and exclusively with $g_{A\gamma}$ were examined separately. Since the AE cross section is proportional to g_{Ae}^2, the number of detected axions is proportional to g_{Ae}^4 and $g_{A\gamma}^2 g_{Ae}^2$ in the first and the second cases, respectively.

Fitting was performed within the 4–20 keV interval by minimizing χ^2. The results of fitting at $g_{Ae} = 0$ and $g_{A\gamma} = 0$ corresponding to the $\chi^2 = 162.0/152$ minimum are represented by the solid curve in Fig. 2. When fitting was performed with the inclusion of AE spectra, the numbers of events in a spectrum corresponding to the χ^2 minimum were negative in both cases. The standard $P(\chi^2)$ profile plotting method was used to determine the upper limit on the number of events in a spectrum. The obtained upper limits on the number of detected axions were 160 and 290 events for the spectra of axions associated with constants g_{Ae} and $g_{A\gamma}$, respectively.

The determined upper limits on the axion count rate allowed us to impose new constraints on constant $|g_{Ae}| \leqslant 4.9 \cdot 10^{-11}$ and the product of constants $|g_{Ae} g_{A\gamma}| \leqslant 1.6 \cdot 10^{-19}\,\mathrm{GeV}^{-1}$. These limits hold true within the 0–4 keV axion mass range; at higher masses, the axion spectrum modification needs to be taken into account.

The obtained limits are model-independent constraints on the coupling constant of an axion (or any other pseudoscalar axion-like particle) with an electron and a photon. The upper limit on $|g_{Ae} g_{A\gamma}|$ has been determined for the first time with the use of the AE reaction, is the most stringent for axion masses above 0.6 eV, and tightens the constraints from [14] by a factor of 2–20. The upper limit on $|g_{Ae}|$ is significantly more stringent than the one reported in [15] and is close to the result obtained under the assumption that solar energy losses due to axions constitute no more than 10% of the energy carried away by neutrinos [6] (Fig. 3).

A search for the absorption of solar axions by krypton atoms via the axioelectric effect was performed. A large gaseous proportional chamber filled with krypton was used to detect photoelectrons, Auger electrons, and X-ray quanta. The low-background setup was located in the underground laboratory of Baksan Neutrino Observatory (Institute for Nuclear Research, Russian Academy of Sciences). New constraints on the coupling constant of an axion with an electron $|g_{Ae}| \leqslant 4.9 \cdot 10^{-11}$ and on the product of coupling constants of an axion with an electron and a photon $|g_{Ae} g_{A\gamma}| \leqslant 1.6 \cdot 10^{-19}\,\mathrm{GeV}^{-1}$ (90% CL) were obtained as a result.

Funding

This study was supported financially by the Russian Science Foundation (project No. 22-22-00017).

Conflict of interest

The authors declare that they have no conflict of interest.

References

[1] R.D. Peccei, H.R. Quinn, Phys. Rev. Lett., **38**, 1440 (1977). DOI: 10.1103/PhysRevLett.38.1440

[2] D.B. Kaplan, Nucl. Phys. B, **260**, 215 (1985). DOI: 10.1016/0550-3213(85)90319-0

[3] M. Srednicki, Nucl. Phys. B, **260**, 689 (1985). DOI: 10.1016/0550-3213(85)90054-9

[4] P.A. Zyla, R.M. Barnett, J. Beringer et al. (Particle Data Group), Prog. Theor. Exp. Phys., **2020**, 083C01 (2020). DOI: 10.1093/ptep/ptaa104

[5] L.M. Krauss, J.E. Moody, F. Wilczek, Phys. Lett. B, **144**, 391 (1984). DOI: 10.1016/0370-2693(84)91285-1

[6] P. Gondolo, G.G. Raffelt, Phys. Rev. D, **79**, 107301 (2009). DOI: 10.1103/PhysRevD.79.107301

[7] D. Kekez, A. Ljubicic, Z. Krecak, M. Krcmar, Phys. Lett. B, **671**, 345 (2009). DOI: 10.1016/j.physletb.2008.12.033

[8] A.V. Derbin, A.S. Kayunov, V.V. Muratova, D.A. Semenov, E.V. Unzhakov, Phys. Rev. D, **83**, 023505 (2011). DOI: 10.1103/PhysRevD.83.023505

[9] J. Redondo, J. Cosmol. Astropart. Phys., **2013**, 008 (2013). DOI: 10.1088/1475-7516/2013/12/008

[10] V. Anastassopoulos, S. Aune, K. Barth et al. (CAST Coll.), Nature Phys., **13**, 584 (2017). DOI: 10.1038/nphys4109
[11] M. Pospelov, A. Ritz, V. Voloshin, Phys. Rev. D, **78**, 115012 (2008). DOI: 10.1103/PhysRevD.78.115012
[12] Yu.M. Gavrilyuk, A.N. Gangapshev, A.V. Derbin, I.S. Drachnev, V.V. Kazalov, V.V. Kobychev, V.V. Kuz'minov, V.N. Muratova, S.I. Panasenko, S.S. Ratkevich, D.A. Semenov, D.A. Tekueva, E.V. Unzhakov, S.P. Yakimenko, JETP Lett., **101** (10), 664 (2015). DOI: 10.1134/S0021364015100069.
[13] Yu.M. Gavrilyuk, A.N. Gangapshev, A.V. Derbin, I.S. Drachnev, V.V. Kazalov, V.V. Kobychev, V.V. Kuzminov, V.N. Muratova, S.I. Panasenko, S.S. Ratkevich, D.A. Tekueva, E.V. Unzhakov, S.P. Yakimenko, JETP Lett., **107** (10), 589 (2018). DOI: 10.1134/S0021364018100090.
[14] K. Barth, A. Belov, B. Beltran et al. (CAST Coll.), J. Cosmol. Astropart. Phys., **2013**, 010 (2013). DOI: 10.1088/1475-7516/2013/05/010
[15] A.V. Derbin, I.S. Drachnev, A.S. Kayunov, V.N. Muratova, JETP Lett., **95** (7), 339 (2012). DOI: 10.1134/S002136401207003X.
[16] D.S. Akerib, S. Alsum, C. Aquino et al. (LUX Coll.), Phys. Rev. Lett., **118**, 261301 (2017). DOI: 10.1103/PhysRevLett.118.261301
[17] A.H. Abdelhameed, S.V. Bakhlanov, P. Bauer, A. Bento, E. Bertoldo, L. Canonica, A.V. Derbin, I.S. Drachnev, N. Ferreiro Iachellini, D. Fuchs, D. Hauff, M. Laubenstein, D.A. Lis, I.S. Lomskaya, M. Mancuso, V.N. Muratova, S. Nagorny, S. Nisi, F. Petricca, F. Proebst, J. Rothe, V.V. Ryabchenkov, S.E. Sarkisov, D.A. Semenov, K.A. Subbotin, M.V. Trushin, E.V. Unzhakov, E.V. Zharikov, Eur. Phys. J. C, **80**, 376 (2020). DOI: 10.1140/epjc/s10052-020-7943-5
[18] Yu.M. Gavrilyuk, A.N. Gangapshev, A.V. Derbin, I.S. Drachnev, V.V. Kazalov, V.V. Kuzminov, M.S. Mikulich, V.N. Muratova, D.A. Tekueva, E.V. Unzhakov, S.P. Yakimenko, JETP Lett., **116** (1), 11 (2022). DOI: 10.1134/S0021364022601075.
[19] O. Straniero, C. Pallanca, E. Dalessandro, I. Domínguez, F.R. Ferraro, M. Giannotti, A. Mirizzi, L. Piersanti, Astron. Astrophys. A, **166**, 644 (2020). DOI: 10.1051/0004-6361/202038775

Translated by D.Safin